Experimental Investigations of Fire Spread from Movable to Fixed Fire Loads in Office Fires

CHI-MING LAI
Department of Civil Engineering, National Cheng-Kung University, Taiwan

MING-JU TSAI
Architecture and Building Research Institute, Ministry of Interior, Taiwan

TA-HUI LIN*
Department of Mechanical Engineering, National Cheng-Kung University, Taiwan

(Received September 8, 2009)

ABSTRACT: Experiments were conducted in a full-scale model office equipped with movable and fixed fire loads to explore the influence of ignition source location (movable fire load(s)) on fire spread. The office space was a brick structure that measured 6 m in interior length, 5 m in width, and 3.3 m in ceiling height, and was equipped with a sprinkler system that was used as a sensor, but not for suppression. The southeast corner of the room featured a 2.1 m × 0.9 m open doorway. Four fire scenarios (four different ignited movable fire configurations) were investigated experimentally. The results show that when the movable fire load is close to the fixed fire load, the fire becomes more intense. The concentrated movable fire load configuration also increases the initial fire intensity.

KEY WORDS: fire spread, fire load, office, flashover.

*Author to whom correspondence should be addressed. E-mail: thlin@mail.ncku.edu.tw
Figures 1–8 appear in color online: http://jfs.sagepub.com

0734-9041/10/06 0539–21 $10.00/0 DOI: 10.1177/0734904110365316

BACKGROUND INFORMATION

A COMPARTMENT FIRE, although complicated and varied, can usually be described by four fire stages, namely, ignition, spread, fully developed, and decay. At the initial ignition stage, the fire source is not affected by the walls of the room, and the heat release rate (HRR) is only controlled by the fire source burning rate. The heat from burning is transferred to the other parts of the room and raises the room temperature through radiation, convection, and conduction. The fire can spread if the heat flux on the nearby pieces of furniture is sufficiently high to cause ignition. Many factors impact the fire's spread at this stage, including the ignition and burning characteristics of the materials, the geometrical configuration of the combustibles, the dimensions and geometry of the room, the sizes and locations of the openings, etc. [1,2]

The plume of hot gases from the fire rises to the ceiling and forms a hot ceiling jet that flows just beneath the ceiling. The hot gases then accumulate under the ceiling to form a so-called upper layer. The radiation flux from the upper layer to the combustibles increases with increasing thickness and temperature of the upper layer. If the fire continues to build, eventually all combustibles in the room will ignite, and the whole room will undergo intensive combustion. At this time, flames usually start to emerge from any openings within the compartment. This point is identified as 'flashover'. There are at least two fundamental definitions of flashover: (1) the occurrence of critical condition in a thermal balance sense; (2) a fluid-mechanical filling process [3]. A significant number of research results have provided data to help predict the occurrence of flashover in room fires. The corresponding prediction methods are based on a simplified mass and energy balance in a fire compartment and have been validated by comparing the results with data from experimental fires [4–9]. Lai et al. [10] proposed a case-based reasoning method to predict the flashover time, based on the *energy filling* concept from the abovementioned fundamental definition (2). Babrauskas et al. [3] collected more comprehensive data regarding flashover times and HRRs at flashover in spaces similar to the ISO 9705 specification. After the occurrence of flashover, the fire is fully developed; high temperatures and high HRRs are often observed in such scenarios. High intensity burning will continue until all the combustible materials are burned out, then the fire will decay.

This study investigated the complicated process by which fire spreads from the movable to the fixed fire loads. We also explored the influence of the ignition locations (movable fire loads) on the fire spread rates

using full-scale compartment fire (office fire) experiments. The fixed fire load consists of wall furnishings, including plywood walls, (hanging) short cabinets, and tall cabinets. The movable fire loads (wood crib(s)) can be used to simulate different ignition configurations with respect to amount and distribution.

EXPERIMENTAL METHOD

Experimental Design

Investigated Model Office

A practical full-scale model office, that measures 6 m in interior length, 5 m in width, and 3.3 m in ceiling height, is used to illustrate actual fire conditions. The southeast corner features a 2.1 m × 0.9 m open doorway. The ceiling is made of a light rigid frame and gypsum board. To better observe the spread of fire, two 2.4 m × 1.2 m fire-resistant windows are located at the north end of the western wall and the west end of the southern wall. The distance between the window and the ground is 0.6 m. See the west and south walls in Figure 1(b) and (c); the overall 3D view is shown in Figure 1(d).

As shown in Figure 2, there are four wall furnishings that serve as fixed fire loads: the plywood wall (item (I) in Figure 2), an upper wood cabinet and lower plywood wall (II), a lower short cabinet and upper plywood wall (III), and a tall wood cabinet (IV). The upper wood cabinet and lower plywood wall (II) and tall wood cabinet (IV) are combined and attached to walls (2) and (4), respectively. The plywood wall (I) and lower short cabinet and upper plywood wall (III) are combined and attached to walls (1) and (3), respectively. The dimensions of all plywood walls are 1.6 m wide, 2.4 m tall, and 4 cm thick. The upper wood cabinet and lower plywood wall (II), and tall wood cabinet (IV) at walls (2) and (4) have a total weight of 102.1 kg. The weight of the plywood wall (I) and of the lower short cabinet and upper plywood wall (III) at walls (1) and (3) is 92.1 kg. The total fire load is approx. 15.4 kg/m^2. Figure 3 shows the interior.

Experimental Scenarios

Four fire scenarios with different ignition source configurations were investigated as indicated in Table 1 and Figure 4. In Test 1, the ignition

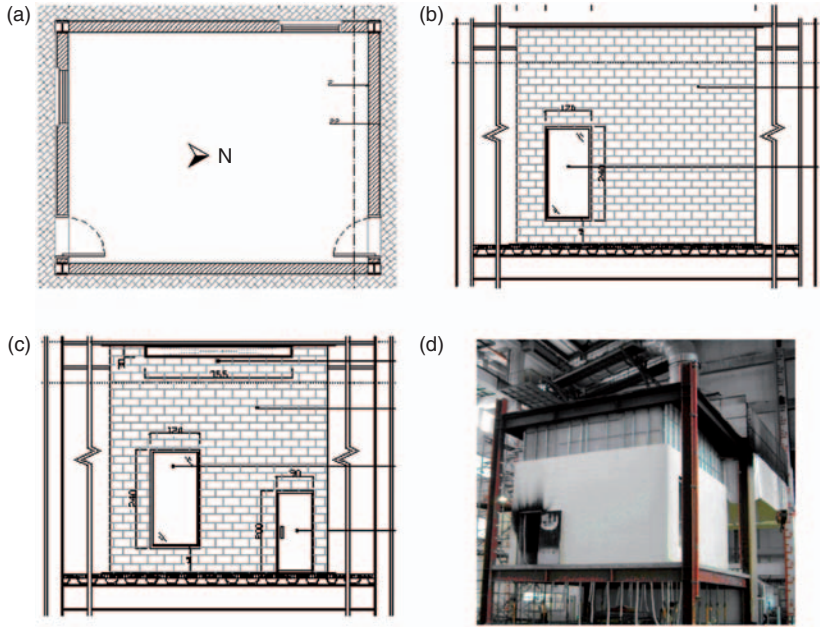

Figure 1. Schematic diagram of the investigated model office (not to scale): (a) plane view, (b) west elevation, (c) south elevation, (d) 3D view (from the northwest).

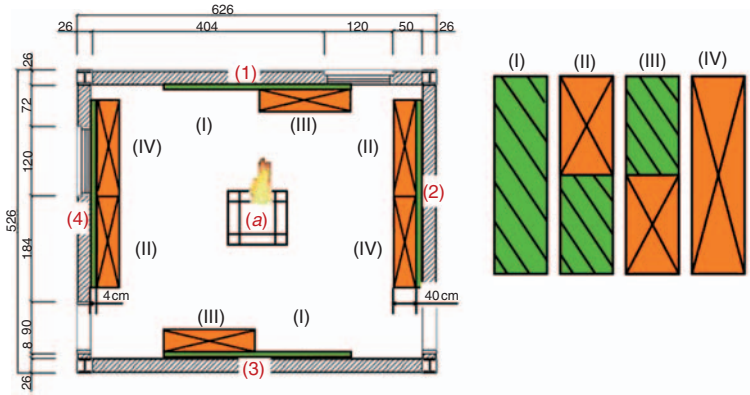

Figure 2. Fixed and movable fire load layout and dimensions.

source is located in the room center. In Test 2, the northeastern and southwestern wood cribs are ignited. In Test 3, the central wooden crib is ignited and the southeastern crib is not. In Test 4, the northwestern wood crib is ignited while the center is not.

Figure 3. The interior of the investigated model office.

Table 1. Experimental scenarios.

Test	Opening	Movable fire load	Fixed fire load	Ignition source
1	Single opening	200 wood strips (a full-size crib) in the center		Central movable fire load (a full-size crib)
2	Single opening	100 wood strips (a half-size crib) in the northeastern and southwestern corners	North/South: tall cabinets and upper hanging cabinets	Northeast and southwest movable fire loads (two half-size cribs)
3	Single opening	100 wood strips (a half-size crib) in the center and in the southwestern corner	East/West: lower cabinets and plywood walls	Central movable fire load (a half-size crib)
4	Single opening	100 wood strips (a half-size crib) in the center and in the northwestern corner		Northwest movable fire load (a half-size crib)

Experimental Procedure

To understand the differences in fire propagation in context of both movable and fixed fire loads, the entire room temperature distributions were measured. Pressure gauges were incorporated within the ends of four independent sprinkling pipes, which were filled with air at high pressure, to confirm sprinkler actuation through sudden pressure drops.

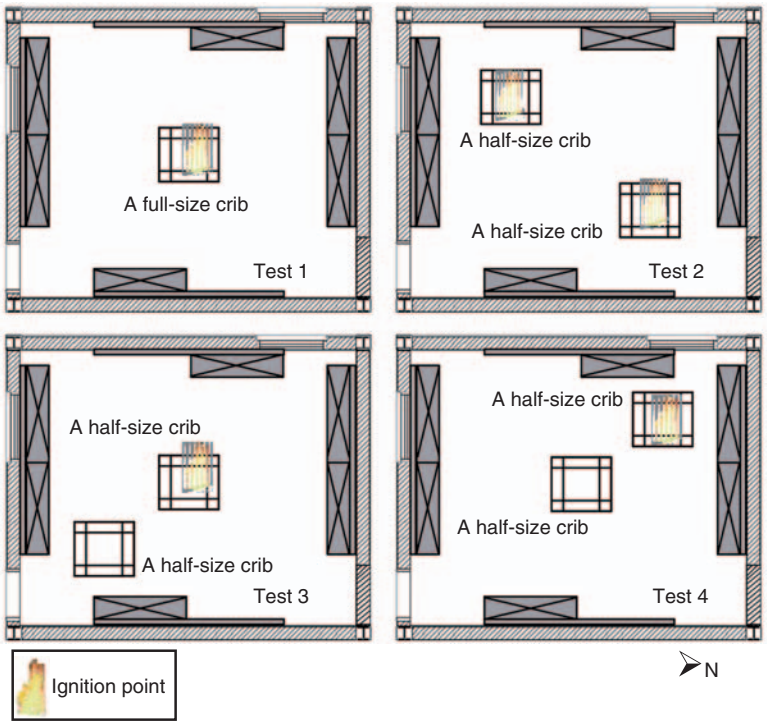

Figure 4. Experimental scenarios.

Ignition

The ignition source was a full or half-size wooden crib, depending on the experimental scenario. Please refer to Table 1 and Figure 4. Each wood strip was 2.4 cm × 3.6 cm × 90 cm. A total of 200 stacked strips make up a full-size wooden crib. They were first dried at 105°C for 24 h and then used in the experiments. Each layer comprised of six wooden strips that were stacked and fixed with nails to avoid premature collapse during the test. Figure 5 illustrates a full-size wooden crib. A pan was placed beneath the wooden crib. Ignition was performed by lighting 1 L of alcohol paste contained in this circular ignition pan.

10 MW Fire Test Facility

Full-scale fire experiments were carried out in a 10 MW fire test facility equipped with continuous online combustion gas analysis. The apparatus is located in the Fire Experiment Center, Architecture &

Figure 5. A full-size wood crib.

Building Research Institute, Ministry of Interior, at the Gueiren Campus of National Cheng-Kung University, Taiwan.

The 10 MW fire test facility consists of a smoke collection hood, smoke collection bend, mixture tube, measurement section, exhaust bend, and exhaust pipe. Large objects or structures can be placed on the floating platform under the hood for testing. Hot gas, smoke, and combustion products are collected by the smoke collection hood, flow vertically through the smoke collection bend, are transferred horizontally into the mixture tube, pass through the measurement section, and exit through the exhaust bend and exhaust pipe. The end of the exhaust pipe is connected to a waste gas treatment system. A large exhaust fan in the waste gas treatment system has a maximum fire gas flow capacity of 30 m^3/s. The investigated model office, shown in Figure 1, is located below the smoke collection hood of the 10 MW fire test facility.

Measurement System

The overall measurement layout is shown in Figure 6. There are a total of 21 thermocouple trees, 4 sprinklers, 1 gas analyzer, and 2 smoke detectors. Round symbols marked by numbers 1–21 are thermocouple trees. Square symbols D1-D4 are smoke detectors; G is a gas analyzer.

Combustion Gas Analysis

The combustion gas continuous online analysis system consists of (1) the gas analysis system (including O_2, CO, CO_2, NO_x, and HC analyzers as well as a gas sampling/calibration system); (2) an optical density analyzer; (3) a flow rate/temperature monitor; and (4) a data processing system.

Temperature Distribution

Each thermocouple tree consisted of a set of K-type thermocouples tied vertically onto a thin iron chain which was attached to the ceiling. A total of 21 thermocouple trees were used in the experiments. The length of each thermocouple tree was 200 cm. The trees were divided into 8 points numbered No. 0 to No. 7 from the ceiling to the floor. The top five thermocouples were spaced 10 cm apart. The spacing between the remaining thermocouples was 50 cm.

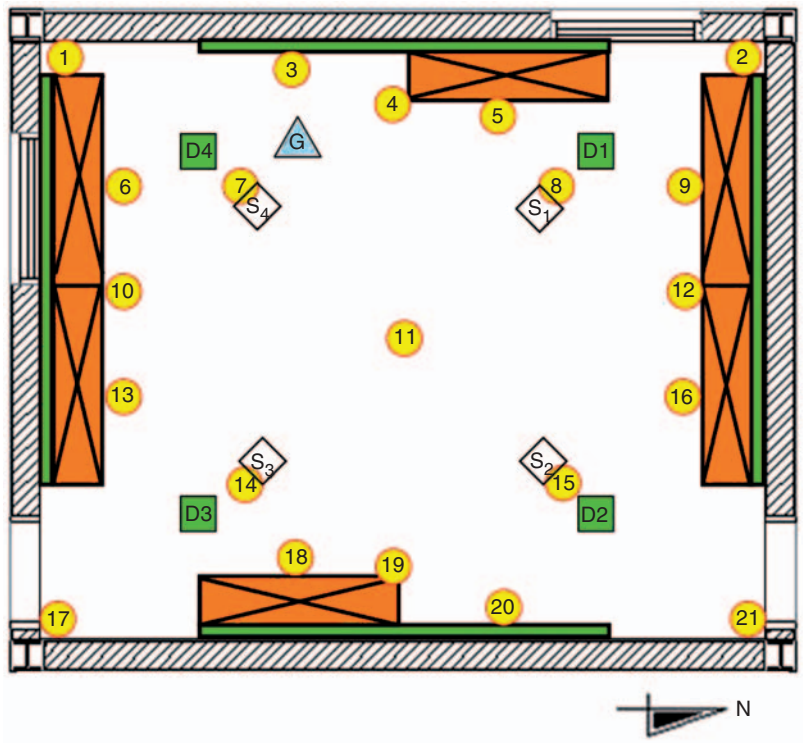

Figure 6. Overall layout of the model office and the measurement apparatus.

Data Acquisition System

A data logger acquired data from the thermocouples, the differential pressure gage, and the flow meter.

Gas Analyzers

The gas analyzer in the investigated model room measured the concentrations of O_2, CO, and CO_2 once per second. The distance of the gas sampling probe from the floor is 180 cm.

Platform Scale

A platform scale, as shown in Figure 7, monitored the mass loss of the wood crib(s). This data was used to calculate the HRR from the wood crib(s).

Video Recording

The experiments were videotaped through a fire-resistant window for subsequent review. In addition, photographs of the fire in the room were taken throughout each test.

Heat Release Rate Analysis

The HRR of combustion products can be calculated in several ways, for example, using methods involving oxygen consumption (OC), CO/CO_2 generation, and gas temperature rise (GTR). This study mainly uses oxygen consumption (OC), which measures the consumption of O_2 or the generation of CO/CO_2 in combustion, and determines the HRR based on the observation that a constant amount of heat is released per

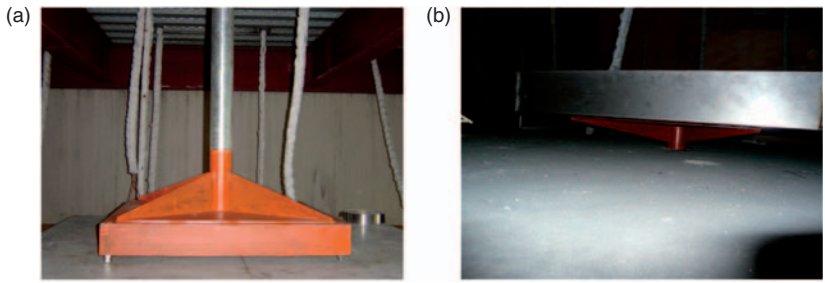

Figure 7. Platform scale for measuring the weight of wood cribs: (a) below the model house, (b) into the model house.

mass unit of O_2 consumed and CO/CO_2 generated [11,12]. The data measured from the gas analyzer is a volume fraction. Due to the analyzer detection requirements, the moisture in the exhaust gas sample must be removed. Gas expansion due to combustion also affects the volume fraction. To obtain a more accurate calculation, this research uses the equations developed by Parker [13] and Janssens [14]. The GTR approach, computing the convective HRR by the enthalpy difference before and after combustion, is also used.

RESULTS AND DISCUSSION

Removable Fire Load at the Center of the Model Office (Test 1)

The entire fire process (Table 2 and Figure 8) in Test 1, from ignition to extinguishing, takes around 1380 s. The fire reaches peak intensity at 600–1000 s. The actuation time of the sprinkler, flashover time, mass loss rate of the crib(s) near the time of flashover, and maximum HRR in each test are summarized in Table 3. Approximately 318 s after ignition in Test 1, S1 is the first sprinkler activated. The hot gas accumulates at the north side, which is the first to be ignited, followed by the east/west plywood walls and then the south wall furnishings. Around 500 s, fire from the movable load propagates to the surrounding fixed load. At 600 s, substantial flame coverage results, and flashover occurs. Figure 9(a) shows the time variation of HRRs in Test 1.

Table 2. Process of the investigated fire in Test 1.

Time (s)	Phenomenon	Pictures
162	The crib bottom was burning	
299	Flame impinged to the ceiling board	Figure 8(a)
318	The S1 sprinkler was first actuated (The sprinklers were filled with high pressure air and not affect the fire development, when leasing)	
332	The S3 sprinkler was actuated	
337	The S2 sprinkler was actuated	
341	The S4 sprinkler was actuated	
500	The tall cabinet in the north was ignited	Figure 8(b)
518	The plywood wall in the east was ignited	Figure 8(c)
558	The tall cabinet in the south was ignited	
600	Flashover occurred	Figure 8(d)
1380	End of experiment	

Heat release from wooden crib (movable fire load) is calculated from the rate of mass loss as measured by the platform scale in Figure 10 (the instantaneous slope of the figure) and shown by the dashed lines in Figure 9. The HRR reaches the first peak, which is mostly associated with the movable fire load. In Figure 11, at 800 s, the temperatures near wall furnishings (TC 4, 10, 12, 19) reach their maximum, and the heat release reaches the maximum value of about 6 MW. The second heat

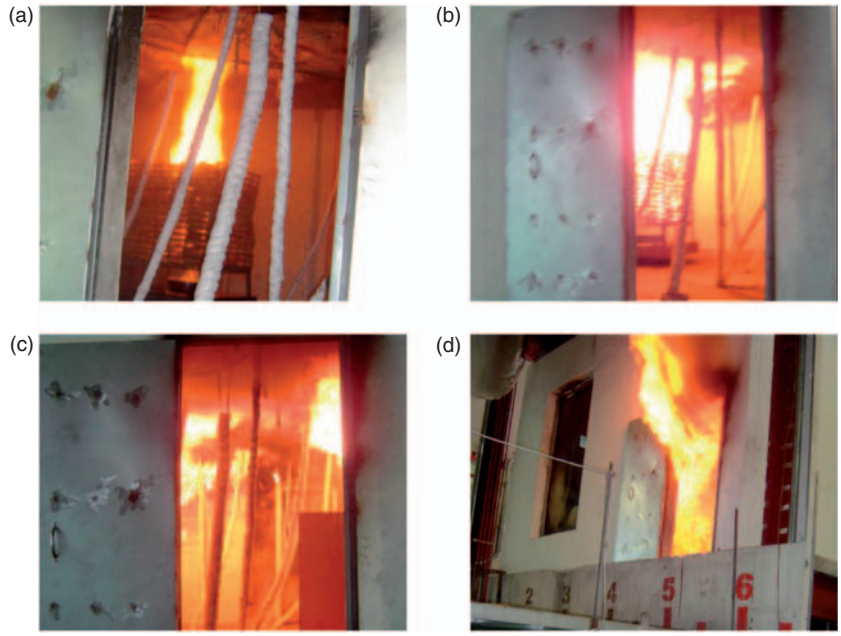

Figure 8. Fire process of Test 1 (observations from southeastern opening): (a) experiment time 299 s, (b) experiment time 500 s, (c) experiment time 518 s, (d) experiment time 600 s.

Table 3. Experimental data.

Test	Sprinkler actuation time (s)	Flashover time (s)	Mass loss rate for the crib(s) near the time of flashover (kg/s)	Max. $\dot{Q}_0$ (MW)
1	318 (S1 sprinkler)	600	0.192	6.0
2	139 (S2 sprinkler)	618	0.197	6.0
3	191 (S3 sprinkler)	Not occurred	n.a.	1.1
4	99 (S1 sprinkler)	450	0.165	7.3

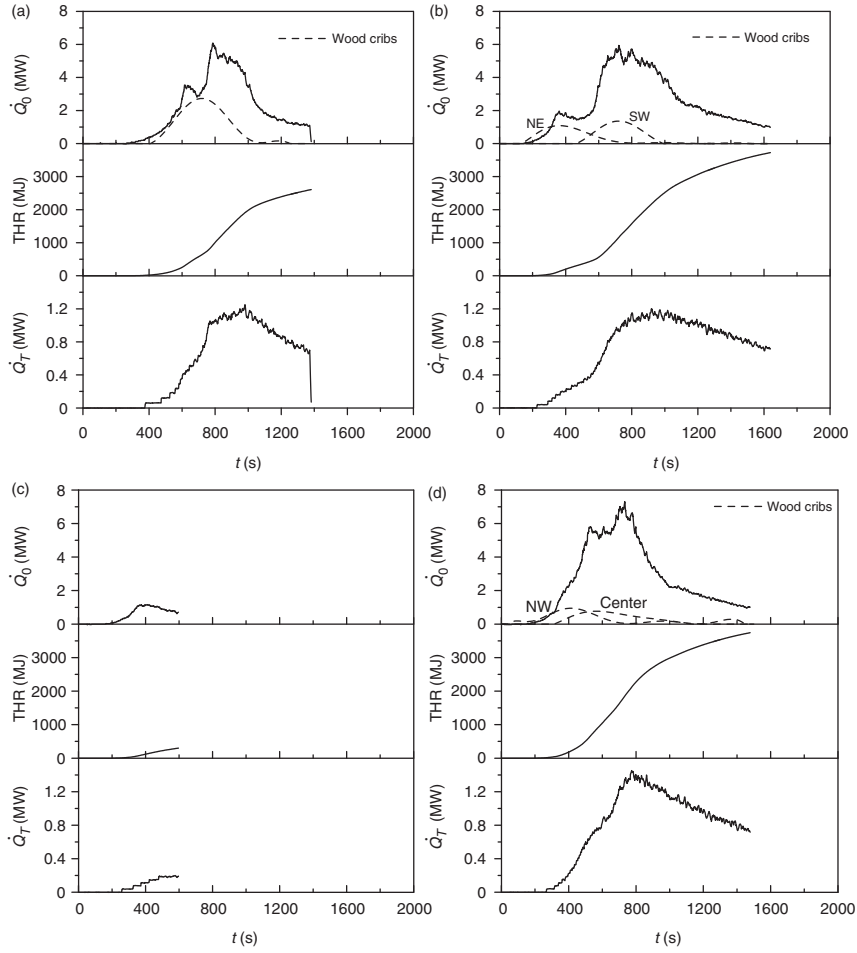

Figure 9. Time variation in heat release rates: (a) Test 1, (b) Test 2, (c) Test 3, (d) Test 4.

release peak is caused by the surrounding wall furnishings. Most thermocouple trees record the highest temperatures between 600 and 700 s. The temperature drops slightly, showing that the fire intensity in the room decreases due to insufficient air supply. This is consistent with the heat release tendency.

In Figure 12, at 550 s, the temperatures of the north and east wall coverings are higher. These two locations are the first to be ignited, a result that is consistent with visual observations and Figure 11(c) and (d). By 600 s, the west side temperature also starts to rise, and the

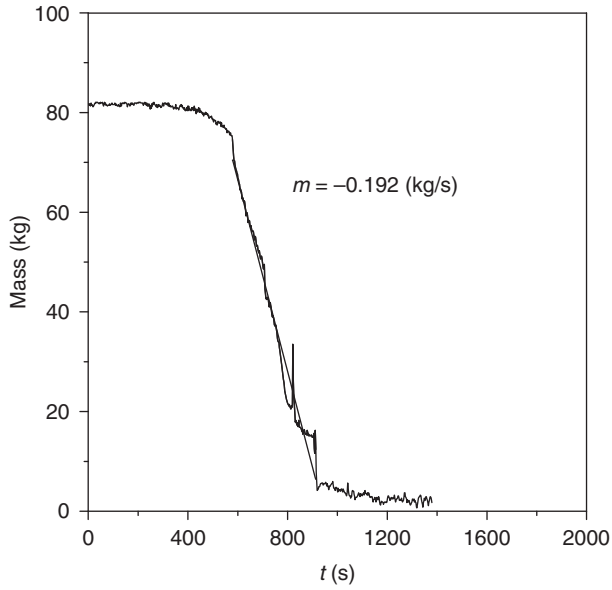

Figure 10. Mass loss rate for the wood crib in Test 1.

west side ignites. The south wall covering closest to the opening is the last to ignite because of slower hot gas accumulation. In Figure 13, at 800 s, the oxygen concentration of the flue gas reaches its lowest point; the originally fuel-controlled combustion subsequently becomes ventilation-controlled. CO and CO_2 concentrations reach their maxima when the heat release is highest, a result that is consistent with Figure 9(a).

Movable Fire Loads at the Northeast and Southwest Corners (Test 2)

At 139 s after the ignition of the movable fire loads in Test 2, the S2 sprinkler is first activated. The movable fire loads are positioned in the northeast and southwest corners. Two wooden cribs are ignited at the same time. Because of the indoor flow pattern, ignition times at the two cribs are not the same. The crib in the northeast corner ignited at 121 s; the southwest crib ignited at 473 s. Sprinkler 2 is the first to be activated. The corner effect concentrates hot gas, and the fire source gets closer to the sprinklers. Therefore, the actuation of the sprinklers in Test 3 is quicker than that in Test 1. At 618 s, fire coverage is severe, and flashover occurs.

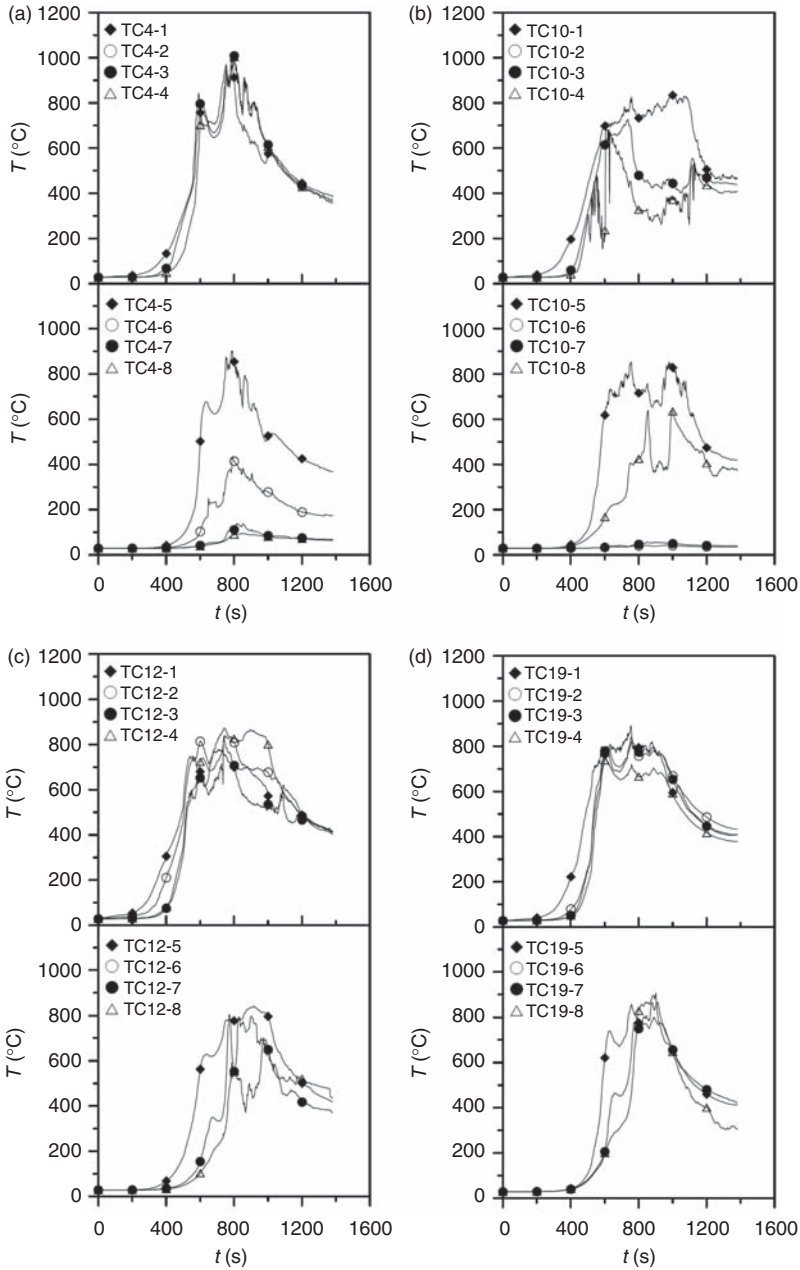

Figure 11. Time variations of the measured temperature of thermocouple trees close to the wall cabinets in Test 1. Temperature distribution at (a) point 4, (b) point 10, (c) point 12, (d) point 19.

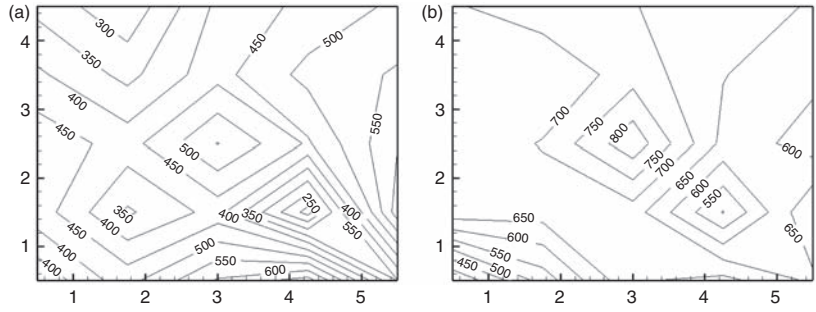

Figure 12. *Isotherm (h = 30 cm: 30 cm from the ceiling) in Test 1: (a) 550 s, (b) 650 s.*

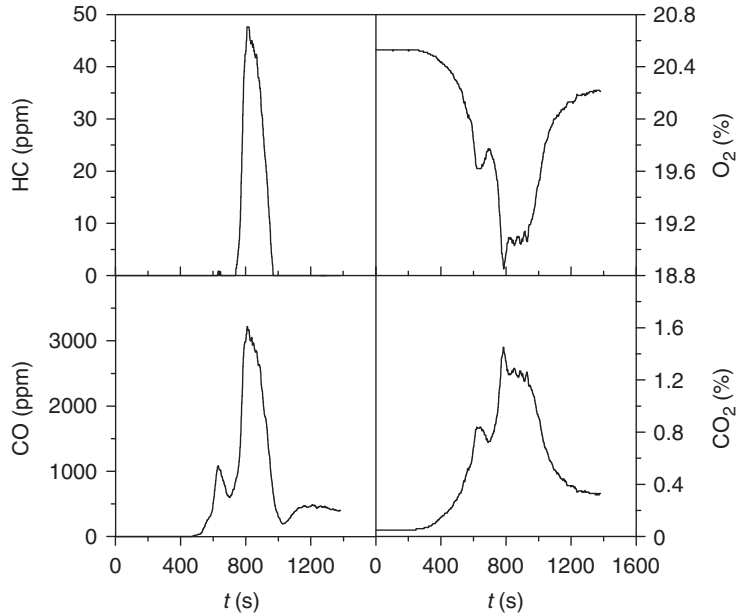

Figure 13. *Flue gas concentrations in Test 1.*

The northeastern wooden crib fire grows more quickly and propagates to the eastern and northern wall furnishings. According to temperature distribution data (not shown, due to the page and figure limits) measured by the thermocouple trees, at 350 s, the wall furnishing temperature has reached 800°C. Figure 9(b) shows the heat release data. Prior to 600 s, most of the heat release is controlled by the wood crib. After the wall furnishings have ignited, heat release is controlled by the

surrounding fixed fire loads. After 800 s, the room oxygen concentration decreases significantly. The room fire transits from fuel-controlled to ventilation-controlled burning, as can be seen from the CO concentration in the flue gas. After 800 s, incomplete combustion is a reality, as indoor oxygen has been consumed.

Movable Fire Loads in the Center and at the Southeast Corner (Test 3)

At 191 s after ignition in Test 3, S3 is the first sprinkler activated. The initial fire caused by the ignited wood crib in the room center did not propagate onto the surrounding wall furnishings and extinguished at about 600 s. Figure 9(c) shows heat release data of Test 3. In Test 1, we learned that when a movable fire load is in the center of a room with a single opening, the critical heat release value of the movable fire load must be 1.2–2.31 MW in order to spread to the surrounding fixed fire load. The maximum HRR in Test 3 is only 1 MW, so the surrounding furnishings cannot be ignited. Thus, flashover was not reached in Test 3 (compared to Test 1) since the ignited crib was only half the size of the crib in Test 1.

Movable Fire Loads at the Center and in the Northwest Corner (Test 4)

At 99 s after ignition in Test 4, S1 is the first sprinkler activated. The wood cribs are placed at the center and in the northwest corner. The wood crib in the northwest is ignited. As the fire source is close to the northwest side, the wall furnishings on the north and west are first ignited at 275 and 289 s. The hot gas layer continues to accumulate. At 375 s, the other movable fire load (wood crib in the room center) is ignited. At 410 s, the smoke layer reaches the top of the short cabinet. By 450 s, flashover occurs.

Figure 9(d) shows the heat release. The full burning period is longer than that recorded in other tests. Heat release during this period is also higher. Ignition sources both in this test and in Test 2 are positioned in the corners. In the north and east, there are plywood walls and a tall cabinet, making smoke layer accumulation more difficult. The fire in Test 2 grows more slowly. In Test 4, on the north and west sides of the ignition source are positioned a hanging upper cabinet and lower cabinet, respectively. Smoke gas is accumulated beneath the hanging upper cabinet and above the lower cabinet, raising the gas temperature and facilitating ignition. Thus, the initial HRR is higher than that of Test 2.

For the temperature distribution as measured by the thermocouple trees (not shown), the TC9 (near the upper cabinet in the north) upper layer temperature grows more quickly than that in TC5 (near the lower cabinet in the west). The hanging upper cabinet in the north ignites earlier than the wall furnishing in the west, consistent with visual observations. In the context of the isotherms (not shown), ignition starts from the north, and fire then spreads to the west and east. By 400 s, the wood crib in the center is ignited, and the temperature in the center of the room 40 cm beneath the ceiling (closer to the flame) is higher than that at 10 cm under the ceiling. At 450 s, the room center temperature reaches 750°C. The high temperature area moves south. Between 500 and 600 s, the room temperature reaches its maximum. At 700 s, oxygen concentration drops to its minimum, and CO and CO_2 concentrations are at their maximum.

Findings

The flashover times and HRRs at flashover of room fire tests from previous works [3,15,16], which used building materials similar to those in Taiwan, are summarized in Table 4. It is obvious that the flashover time is concentrated. The room dimensions, summarized in Table 4, are comparable to those specified in ISO 9705. The room in the ISO standard has a volume of 20.7 m^3. The volume of the investigated model office is 99 m^3, which is 4.78 times that of the ISO 9705 room. Experiment No. 10 in Table 4 uses building materials similar to those in this study. The flashover time and HRR at flashover for that experiment

Table 4. Selected flashover times and heat release rates at flashover of the room fire tests from previous studies [3,15,16].

No.	Building materials	Flashover time(s)	HRRs at flashover (kW)
1	Plywood walls, gwb[a] ceiling, mixed furniture (1)[15]	117	1030
2	Plywood walls, gwb ceiling, mixed furniture (2)[15]	114	1190
3	Plywood walls, gwb ceiling, mixed furniture (3)[15]	108	1880
4	Plywood walls, gwb ceiling, mixed furniture (4)[15]	106	1610
5	gwb walls and ceiling, mixed furniture [15]	100	2420
6	Paper wall covering on particleboard [16]	133	980
7	Particle board (1)[16]	138	950
8	Particle board (2)[16]	146	1160
9	Particle board (different burner program)[16]	141	1970
10	Concrete walls, gwb ceiling, mixed furniture [15]	178	1620

[a]gwb: paper-faced gypsum wallboard.

are 178 s and 1620 kW, respectively. The 2870, 2700, and 3000 kW HRR at flashover measured at Test 1, Test 2, and Test 4 are 1.77, 1.67, and 1.85 times 1620 kW (experiment No. 10 in Table 4), respectively. According to the second basic definition in which flashover is defined as a 'fluid-mechanical filling process' [3,10], the '*energy filling*' ability in Scenario 1 should be 2.7 (4.78/1.77), 2.87 (4.78/1.67), and 2.58 (4.78/1.85) times higher than that presented in Table 4. The possible flashover time in Test 1, Test 2, and Test 4 from the above inference should be 481 s (178×2.7), 511 s (178×2.87), and 460 s (178×2.58), which is comparable to the measured flashover time (600, 618, and 450 s at Test 1, Test 2, and Test 4, respectively). This type of case-based reasoning method is tested again and worth studying further to explore its potential in room fire science.

From Figure 9, it is clear that the measured HRR reaches the first plateau in the periods from 550 to 600 s and about 400 s in Test 1 and Test 4, respectively. It can be approximated by $750\,A\sqrt{H}$ (=2054 kW), as found in Lee et al. and Ohmiya et al. [17,18], where A is the opening (generally, door) area (1.89 m^2) and H is the opening (generally, door) height (2.1 m). The plateau was not clearly identified in Test 2 and reached in Test 3. The same trend can be observed from the gas temperature distributions. During the intermediate plateau, flames only existed inside the model office, with excess pyrolysate escaping outside the room prior to ignition. After ignition, the measured HRR increased until reaching a steady state at about 6 MW in both Test 1 and Test 4.

For the investigated ventilation-controlled fires (Test 1, Test 2, and Test 4) (near the times of flashover), the fuel mass loss rates were 0.192, 0.197, and 0.165 (kg/s), respectively (Table 3). These were reasonably consistent with the $0.1\,A\sqrt{H}$ value (0.2 kg/s) as calculated using Kawagoe's equation [19] for pyrolysis in under-ventilated fires. This result supports the argument that this relation ($\dot{m}_T = 0.1A\sqrt{H}$, where $\dot{m}_T$ is mass pyrolysis rate of fuel) is independent of the properties of the fuel in full-scale room fires. The HRR at flashover, with respect to the compartment surface area (A_T) and the vent size (expressed as $A\sqrt{H}$), ($A_T/A\sqrt{H}$, HRR/$A\sqrt{H}$), is (56.37, 1300). These results are consistent with the trend introduced in Babrauskas et al. [3].

CONCLUSION

When the movable fire load is close to the fixed fire load, the fire intensifies, as shown in Test 2 and Test 4. In Test 2, the movable fire loads are placed in the northeast and southwest corners, with two

wooden cribs ignited simultaneously. In Test 4, to the north and west of the fire source are positioned a hanging cabinet and a short cabinet, closer to the fire source. Smoke gas accumulates beneath the hanging cabinet and above the short cabinet, increasing the temperature and facilitating ignition. The initial heat release is greater. The concentrated movable fire load configuration also aids initial fire intensification.

It is clear that the measured HRR reaches a plateau and is approximately equal to 750 $A\sqrt{H}$ (=2054 kW), as found in Lee et al. and Ohmiya et al. [17,18]. The same trend can be observed from the gas temperature distributions. From the investigated ventilation-controlled fires, the fuel mass loss rates are consistent with the 0.1 $A\sqrt{H}$ (=0.2 kg/s) calculation from Kawagoe's equation [19] for pyrolysis in under-ventilated fires. Based on the *energy filling* concept from the fundamental definition of flashover as a 'fluid-mechanical filling process', it is possible to predict a reasonable flashover time by comparing room volume and HRRs at flashover with previous studies that featured similar building materials and fire loads. This kind of case-based reasoning method will be an object of further study.

NOMENCLATURE

D = smoke detector
G = gas analyzer
GTR = gas temperature rise method
OC = oxygen consumption method
$\dot{Q}$ = heat release rate (MW)
S = sprinkler
TC = thermocouple
THR = total heat release (MJ)

Subscripts and superscripts

I = location of TC (i=1–21), smoke detector (i=1–4), or sprinkler (i=1–4)
O = heat release rate determined by OC
T = convective heat release rate determined by GTR

ACKNOWLEDGMENTS

Support from the Architecture and Building Research Institute, Ministry of Interior, Taiwan is gratefully acknowledged.

REFERENCES

1. Lai, C.M., Su, H.C., Chen, C.J., Tsai M.J., Tzeng, C.T. and Lin, T.H. (2010). Influence of Fire Source Locations on the Actuation of Wet-type Sprinklers in an Office Fire, *Building and Environment*, **45**(1): 107–114.
2. Lai, C.M., Chen, K.J., Chen, C.J., Tzeng, C.T. and Lin, T.H. (2010). Influence of Fire Ignition Locations on the Actuation of Smoke Detectors and Wet-type Sprinklers in a Furnished Office, *Building and Environment*, **45**(6): 1448–1457.
3. Babrauskas, V., Peacock, R.D. and Reneke, P.A. (2003). Defining Flashover for Fire Hazard Calculations: Part II, *Fire Safety Journal*, **38**: 613–622.
4. Babrauskas, V. (1980). Estimating Room Flashover Potential, *Fire Technology*, **16**(2): 94–103.
5. McCaffrey, B.J., Quintiere, J.G. and Harkleroad, M.F. (1981). Estimating Room Temperatures and the Likelihood of Flashover using Fire Data Correlations, *Fire Technology,* **17**(2): 98–119.
6. Mowrer, F.W. and Williamson, R.B. (1987). Estimating Room Temperatures from Fires along Walls and in Corners, *Fire Technology,* **23**(2): 133–145.
7. Thomas, P.H. (1981). Testing Products and Materials for their Contribution to Flashover in Rooms, *Fire and Materials,* **5**: 103–111.
8. Deal, S. (1994). *NISTIR 5486. Technical Reference Guide for FPEtool Version 3.2,* National Institute of Standards and Technology, Gaithersburg, MD, USA.
9. Foote, K.L., Pagni, P.J. and Alvares, N.J. (1986). Temperature Correlations for Forced-Ventilation Compartment Fires, In: *Fire Safety Science – Proceedings of the First International Symposium*, *International Association for Fire Safety Science*, pp. 139–148, Hemisphere Publishing, Washington, DC.
10. Lai, C.M., Ho, M.J. and Lin, T.H. (2009). Experimental Investigations of Fire Spread and Flashover Time of Office Fires, *Journal of Fire Sciences*.
11. Thornton, W. (1917). The Relation of Oxygen to the Heat of Combustion of Organic Compounds, *Philosophical Magazine and Journal of Science*, **33**: 196–203.
12. Huggett, C. (1980). Estimation of Heat Release by means of Oxygen Consumption Measurement, *Fire and Materials,* **12**: 61–65.
13. Parker, W. (1982). *Calculation of the Heat Release Rate by Oxygen Consumption for Various Applications*, NBSIR 81-2427, National Bureau of Standards, Gaithersburg, MD.
14. Janssens, M. (1991). Measuring Rate of Heat Release by Oxygen Consumption, *Fire Technology*, **27**: 234–249.
15. Fang, J.B. and Breese, J.N. (1980). *Fire Development in Residential Basement Rooms*, NBSIR 80-2120, National Bureau of Standards, Gaithersburg, MD.
16. Sundström, B. (1986). *Full Scale Fire Testing of Surface Materials* (SP-RAPP 1986:45), Swedish National Testing Institute, Borås.

17. Lee, Y.P., Delichatsios, M.A. and Silcock, G.W.H. (2007). Heat Fluxes and Flame Heights in Facades from Fires in Enclosures of Varying Geometry, *Proceedings of the Combustion Institute,* 31: 2521–2528.
18. Ohmiya, Y., Tanaka, T. and Wakamatsu, T. (1998). A Room Fire Model for Predicting Fire Spread by External Flames, *Fire Science and Technology*, **18**(1): 11–21.
19. Kawagoe, K. and Sekine, T. (1963). Estimation of Fire Temperature Rise Curves in Concrete Buildings (Part 2), *Architectural Institute of Japan*, **86**: 40–47.

BIOGRAPHIES

Chi-Ming Lai

Chi-Ming Lai received his Bachelors and Masters degree of Mechanical Engineering from National Cheng-Kung University (NCKU) in Taiwan, and PhD of Architecture at the same university. He is currently an Associate Professor at the Department of Civil Engineering, NCKU. His research activities cover a wide spectrum of topics in the building physics, fire science, energy and smart living space.

Ming-Ju Tsai

Ming-Ju Tsai completed his PhD degree in Construction Engineering from National Taiwan University of Science and Technology. He is the Director of Fire Experiment Center, Architecture & Building Research Institute, Ministry of Interior, Taiwan. His research interest includes building fire, fire resistance test (structural parts, fire door, fire window, etc.) for buildings and heat release rate research for building materials.

Ta-Hui Lin

Ta-Hui Lin received his PhD degree in Mechanical Engineering from Northwestern University, USA. He is currently a distinguished University Professor and Chair of Mechanical Engineering Department at National Cheng-Kung University (NCKU) in Taiwan. His research interests include basic combustion researches (gaseous combustion, droplets and spray combustion), applied combustion researches (gas stoves, IC engines, industrial furnaces and boilers) and combustion related researches (energy utilization, air pollution control and fire science).